EUROFUSION NJOC-CP(16) 15502

C Sozzi et al.

Detection of Neoclassical Tearing Modes in DEMO using the Electron Cyclotron Emission

Preprint of Paper to be submitted for publication in Proceedings of 29th Symposium on Fusion Technology (SOFT 2016)

This work has been carried out within the framework of the EUROfusion Consortium and has received funding from the Euratom research and training programme 2014-2018 under grant agreement No 633053. The views and opinions expressed herein do not necessarily reflect those of the European Commission.

Detection of Neoclassical Tearing Modes in DEMO using the Electron Cyclotron Emission

N. Rispoli[a,*], L. Figini[a], D. Micheletti[a], D. Farina[a], S. Nowak[a], C. Sozzi[a]

[a]*Istituto di Fisica del Plasma - CNR, Milano, Italy*

Abstract

Tokamak plasmas, in low safety factor scenarios, are prone to magnetohydrodynamic (MHD) low m,n instabilities which may affect the energy and particle confinement time and possibly lead to disruptive plasma termination. In presently operating tokamaks high space resolution ($\sim$ 2cm) and high time resolution ($0.01 - 0.1$ms) Electron Cyclotron Emission (ECE) diagnostics are embedded in the control loop finalized to MHD control, often in synergy with pick-up coils sensitive to the magnetic fluctuations. Microwave diagnostics have plasma-facing components that are electrically passive, have metal body and are mechanically fixed. Such characteristics of robustness and reliability are promising features but it has not been proved yet that the ECE diagnostic performances are good enough for this task in the DEMO reactor. Moreover, the same kind of solution used today plant might be beyond reach in a fusion power, given the much higher neutron fluence ($15 - 20$ times of ITER) which makes unlikely the regular operation of detectors close to the vessel wall like pick-up coils. One specific task that the ECE diagnostics should accomplish in DEMO is then the prompt detection of Neoclassical Tearing Modes without the auxiliary detection capabilities of fast magnetic diagnostics. An assessment of this capability can be performed simulating the ECE temperature signals [1] associated with NTM perturbation [2] and then processing them with a detection algorithm [3] without using any other diagnostic signal, also taking into account noise sources. The results of such assessment referred to the EU-DEMO1-2015 scenario is reported in this paper, showing that extraordinary mode ECE in 2^{nd} harmonics seems to have enough space resolution in the region interested by 3/2 and 2/1 NTMs.

Keywords:
`Neoclassical tearing mode`
`Time-dependent simulation`
`Tokamak`

1. Introduction

Microwave diagnostics have plasma facing components (antennas) that are electrically passive, have metal body and are mechanically fixed. Such characteristics of robustness and reliability are a promising feature but the diagnostic performances in term of achievable space resolution and profile coverage in the high temperature and density conditions of the DEMO reactor need to be assessed. In presently operating tokamaks high space resolution ($\sim$ 1cm, which is $\sim 0.01^{*}$minor radius) and high time resolution ($0.01 - 0.1$ms, which is $\sim$ reciprocal of the diamagnetic frequency) Electron Cyclotron Emission (ECE) diagnostics are embedded in the control loop finalized to Magnetic Hydro Dynamic (MHD) control, often in synergy with pick-up coils sensitive to the magnetic fluctuations. The main task that the ECE diagnostic should accomplish in DEMO is the prompt detection of instability without auxiliary magnetic diagnostics, in particular: NTM island must be detected when it is only few cm wide and its localization must be precise enough to obtain accuracy comparable with to the island size. An optimized Detection Algorithm (DA) is mandatory. To evaluate the performance of the DAs a simulation tool, like [2], has been developed and presented in section 2. The DAs considering in this analysis are described in the section 3. The main results of performance evaluation, referred to the EU-DEMO1-2015 scenario, are reported the main results in section 4.

2. Simulation Tool

The simulation tool has been realized in the graphic environment Matlab/Simulink. In the figure 1 is shown a simplified diagram of the numerical scheme, it has been composed by three main blocks: first block compute to the island grow time evolution; second block is used to compute (off-line) the 3D map of the temperature perturbation relative to island presence; third block is devoted to compute the time dependent EC emission relative to is-

*Corresponding author
Email address: `natale.rispoli@ifp.cnr.it` (N. Rispoli)

land evolution. A brief description of main characteristics of three blocks are reported below.

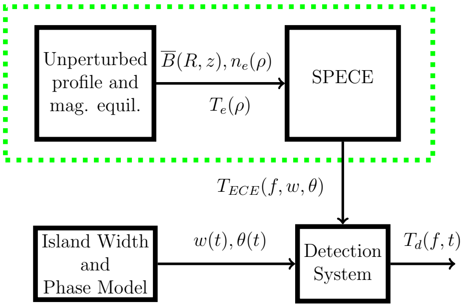

Figure 1: Simplified scheme of simulation tools

2.1. Island width and phase evolution

The time evolution of the island is evaluated using a set of 2 equations for the mode width (Generalized Rutherford Equation, G.R.E.) and for the mode frequency ([4] and reference within). The G.R.E. includes terms not depending on the mode frequency (linked to the mode stability parameter, to the bootstrap current and to the stabilizing effect of the field curvature), terms depending on the frequency (related to the ion polarization current and to the effect of the resistive wall) and terms depending on the injected external power (EC heating and current drive, not used in our case). The mode frequency equation includes the effect of three torques: the electromagnetic braking torque due to the eddy currents, the viscous torque with anomalous viscosity and the inertial braking torque due to the growing momentum of inertia.

2.2. Magnetic and Temperature perturbation

In presence of a magnetic island the magnetic equilibrium loses its axis symmetry and it assumes a 3-d configuration, depending on the three coordinates: minor radius, poloidal and toroidal angles. A simple model for such 3-d magnetic perturbation has been assumed in [5]. This model has been used for the first time in [2] for the evaluation of the asymmetric perturbation of the electron temperature across the rational surface, and its impact on NTMs detection with ECE.

The ECE spectra in presence of a helicoidal temperature perturbation at a given rational surface (q=2) has been modelled with the SPECE code[1], for a set of island sizes spanning the whole range between zero-sized island and full-size saturated island and different phases ξ_0 , i.e. angular positions, of the island. The resulting data set, which describes the perturbed temperature profiles corresponding to a set of island sizes and phases has been used by detection system.

2.3. Detection system

The detection system combine the static results of SPECE with the dynamic data of island evolution to calculate the ECE signals as function of time. Moreover the detection system add two Gaussian white noises on each ECE channel. The first one is the Thermal Noise (ΔT_n), where its amplitude is related to the radiometer video bandwidth (B_v), the intermediate frequency bandwidth (B_{IF}) and the mean temperature of each ECE channel. The second one is the Instrumental Noise (ΔT_i), which takes into account the noises introduced by the transmission line and by the radiometer electronic components [6]. The resulting signals (with noise), mimicking the typical output of a multichannel radiometer, are used as input for the detection algorithm.

3. Detection Algorithms

The algorithm by Berrino et al. [3], that use only ECE signals, has been used for island location detection. Using the correlation between adjacent frequency channels, it detects the oscillation phase jump on the temperature signal on opposite sides of the rational flux surface.

With this algorithm when two ECE channels are partially/completely located in a region at constant temperature the detection capability of the algorithm decreases. This can be happen for large island width or when one of the ECE channels is locate too near the center of island.

Introducing a new type of correlation, an Enhanced Detection Algorithm has been realized to overcome these potential problems. As mentioned previously the Berrino Detection Algorithm calculates the correlation between two adjacent channels, otherwise the new algorithm also takes account of correlation information between non-adjacent channels, as reported in the formula below:

$$C_i^b = c(\overline{\delta T}_i, \overline{\delta T}_{i+1}) + c(\overline{\delta T}_{i-1}, \overline{\delta T}_{i+1}) \quad (1)$$

$$C_i^a = c(\overline{\delta T}_i, \overline{\delta T}_{i+1}) + c(\overline{\delta T}_i, \overline{\delta T}_{i+2}) \quad (2)$$

for $i = 2, \ldots, N_{ECE} - 2$, where $\overline{\delta T}$ is normalized temperature oscillation and $c(\cdot, \cdot)$ is simple correlation between two channels.

4. Results

The two algorithms have been tested on DEMO1 scenario [7] at O-mode and X-mode frequencies for signals collected through the equatorial line of sight. The chosen parameters for the detection system simulation are $B_{IF} = 500MHz$, $B_v = 2kHz$, $1/\tau_{samp} = 2B_v = 4kHz$, $\Delta T_i = 8.3eV$ and $\Delta T_n = T/\sqrt{B_{IF} * \tau_{samp}}$. In this conditions the total noise level at $q = 2$ location is $\approx 21eV$. The radiometer frequencies and island location are reported in table 1.

In figure 2 a comparison, at O-mode frequencies, between the correlations is shown, where the 4^{th} ECE channel frequency is very close to island center. The main effect of the EDA is the correlation signal amplification near the island position, that result in a better detection accuracy.

Figures 3 and 4 show the output of the identification algorithm and the respectively accuracy, as seen through

	$O - Mode$	$X - Mode$
N. channels	15	18
f_{ECE} $[GHz]$	$125 - 140$	$250 - 267$
f_{isl} $[GHz]$	127.9	256.5

Table 1: Multichannel radiometer characteristic and island frequency location

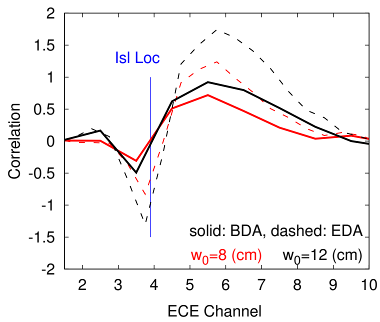

Figure 2: Correlation results Vs Channels

the temperature perturbation at the OM1 frequency and XM2, for island located on $q = 2$ rational surface and initial island seed $w_0 = 3[cm]$ and rotation frequency $\omega_0 = 420[kHz]$.

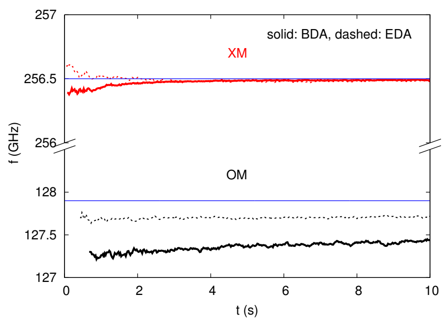

Figure 3: Time evolution of the island frequency location identification

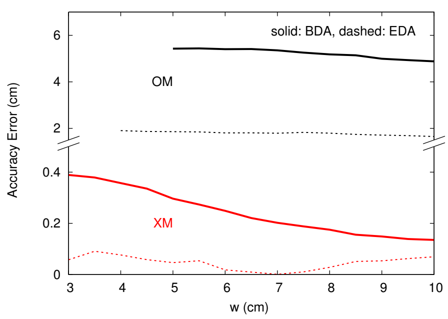

Figure 4: Time evolution accuracy error on island location identification

Figure 3 show successful detection of island when its width exceeds: $w \approx 5/3cm$ for O-Mode/X-Mode for BDA; $w \approx 4/3cm$ for O-Mode/X-Mode for EDA. Moreover at O-Mode the BDA exhibits an accuracy lack ($\Delta r \approx 5[cm]$), where the EDA is faster than BDA and has better accuracy, but is not suitable for control yet ($\Delta r \approx 2[cm]$). Figure 3 also show that at X-Mode both DAs exhibit very low detection latency ($\Delta t_l < 0.1s$).

Figure 4 show that at X-Mode both DAs exhibit very good accuracy ($\Delta r < 0.4[cm]$) for every island width. In this condition the EDA exhibits four times better accuracy than the BDA ($\Delta r < 0.1[cm]$).

The radiometer's video filter, with bandwidth B_v, limits the highest amplitude oscillation frequency that can be detected on ECE signals. Some tests have been done with different B_v in order to identify latency trend versus the maximum island rotation frequency (mode) detectable by the algorithm, the results are reported in figure 5. Simulation make in evidence that, in oder to have low detection latency, B_v should be chosen as small as possible, consistently with the required time resolution to detect the maximum frequency of island rotation, that for the considered case limit the $B_v \approx 2kHz$ which result in at least 10 samples for every oscillation.

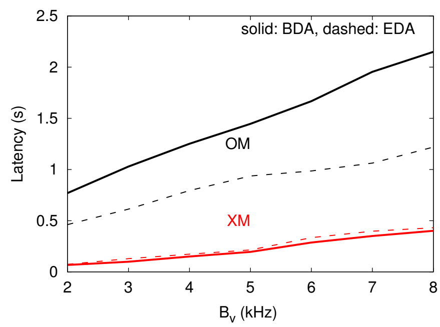

Figure 5: Detection latency vs B_v

5. Conclusions

To test detection algorithm a Simulink/Spece simulation tool has been realized and the evaluation of the diagnostic capability of ECE in DEMO1 scenario has been performed.

The detection's limits of algorithm by Berrino [3] had been shown and an enhanced detection algorithm has been proposed and tested on OM1 and XM2. On OM1 range of frequency, the new algorithm is faster than the old one and has better accuracy, but is not suitable for control yet. For both algorithms the XM2 range of frequency is suitable for NTM fast and accurate identification using an antenna mounted close to the equatorial plane. The evaluations performed confirm the ECE diagnostic potential for NTM control purposes. The considerations here reported apply to the plasma scenario described in [7].

References

[1] D. Farina, L. Figini, P. Platania, C. Sozzi, AIP Conference Proceedings 988 (2008) 128–131. URL: `http://scitation.aip.org/`

content/aip/proceeding/aipcp/10.1063/1.2905053. doi:http://dx.doi.org/10.1063/1.2905053.

[2] H. van den Brand, M. de Baar, N. L. Cardozo, E. Westerhof, Nuclear Fusion 53 (2013) 013005. URL: http://stacks.iop.org/0029-5515/53/i=1/a=013005.

[3] J. Berrino, E. Lazzaro, S. Cirant, G. D'Antona, F. Gandini, E. Minardi, G. Granucci, Nuclear Fusion 45 (2005) 1350. URL: http://stacks.iop.org/0029-5515/45/i=11/a=016.

[4] E. Lazzaro, S. Nowak, Plasma Physics and Controlled Fusion 51 (2009) 035005. URL: http://stacks.iop.org/0741-3335/51/i=3/a=035005.

[5] J. Yang, Q. Yu, S. Zhu, G. Zhuang, Physics of Plasmas 16 (2009). URL: http://scitation.aip.org/content/aip/journal/pop/16/9/10.1063/1.3240329. doi:http://dx.doi.org/10.1063/1.3240329.

[6] Pandya, Hitesh Kumar B., Udintsev, V.S., Vayakis, G., Austin, Max, EPJ Web of Conferences 32 (2012) 03005. URL: http://dx.doi.org/10.1051/epjconf/20123203005. doi:10.1051/epjconf/20123203005.

[7] DEMO1 Reference Design 2AQ5GP v1.0 (2015). URL: https://idm.euro-fusion.org/?uid=2AQ5GP.

Acknowledgment

This work has been carried out within the framework of the EUROfusion Consortium and has received funding from the Euratom research and training programme 2014-2018 under grant agreement No 633053. The views and opinions expressed herein do not necessarily reflect those of the European Commission.